Direct Observation of Switching Processes in Permalloy Rings with Lorentz Microscopy

T. Uhlig* and J. Zweck

Institut für Experimentelle und Angewandte Physik, Universität Regensburg, 93040 Regensburg, Germany

(Received 27 February 2004; published 20 July 2004)

To achieve a deeper understanding of the switching process of magnetic Permalloy rings, Lorentz electron microscopy (LTEM) is used for the first time to image the magnetic configuration of such rings under applied external field conditions. Because of the exceptionally high lateral resolution we find two clearly distiguishable wall configurations present in the so-called "onion state." Furthermore, we show that a bias field present during a remagnetization cycle prevents the rings from transforming into a flux closure state, in which case remagnetization is a pure domain wall motion process.

DOI: 10.1103/PhysRevLett.93.047203 PACS numbers: 75.60.Jk, 68.37.Lp

To continue the rapid increase of the storage density in random access memory (RAM) chips, new data storage concepts have been developed in the last few years. One of the most cited research areas is connected with the possibility of replacing the conventional DRAM (dynamic RAM) with magnetic RAM devices (MRAMs). As every bit should be stored in a small stack consisting of two separated magnetic layers, the storage density depends on the minimal distance between two stacks which is defined by the critical stray field value of adjacent cells. Therefore increasing the packing density corresponds with minimizing the stray fields. This makes circular dots favorable, as these elements form flux closure states without an external stray field in remanence. The information can then be stored in the chirality of the vortex. However, the vortex center is a high energy density region within the vortex. After elimination of the center area, in the remaining ring structure a flux closure pattern forms as well, which is more stable than in circular dots because of energetic reasons as mentioned before. Ring structures have been proposed as possible MRAM elements [1].

The switching mechanisms of small rings have been studied extensively by theoretical simulations which were compared with experiments performed by, e.g., magnetic force microscopy (MFM) [2] or magneto-optical Kerr effect (MOKE) [3,4]. However, high resolution imaging of the magnetic domain structures could so far only be performed in zero field with photoemission electron microscopy (PEEM) and scanning electron microscopy with polarization analysis (SEMPA) [5]. In this work we present high resolution pictures taken *in situ* with applied external field and recorded by differential phase contrast microscopy (DPC) [6], which is an advanced technique of Lorentz microscopy [7]. This enables us to investigate also remagnetization processes and to image domain wall profile details as well.

We use a transmission electron microscope to image the magnetic induction of the ring structures with high spatial resolution (5 nm), even in the presence of external magnetic fields. The external in-plane field is generated by tilting the specimen holder in the vertical field of the objective lens which is about 170 kA/m. Thus, every in-plane field is connected with an out-of-plane component, which has only a negligible effect on the specimen due to the strong demagnetizing field of the thin film microstructures [8]. For our experimental setup the accuracy in the applied field is 0.2 kA/m, which can be deduced from the angle uncertainty of the stage of 0.02°.

We use DPC as a high resolution magnetic imaging technique. A focused electron beam is scanned across the specimen. The Lorentz force connected to the magnetic induction of the specimen causes a local deflection of the electron beam which can be detected in the back focal plane of the imaging lens by an annular four quadrant detector [9] as a shift of the beam disk (see Fig. 1). By taking the difference signal of two opposite detector segments, every scanned point is characterized by two values corresponding to the x and the y component of the magnetic induction. Both components can be displayed either as two different gray value images, where the direction of the plotted induction component is indicated by the mapping direction arrow or as a vector field plot, where the vectors represent the reconstructed magnetic induction [10].

A remotely controlled Philips/FEI Tecnai F30 equipped with a field emission gun and a custom made four quadrant detector is used in this work. Magnetic

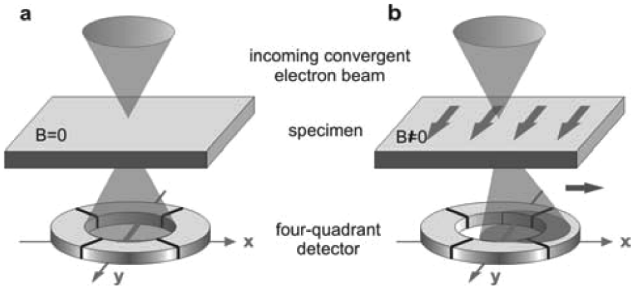

FIG. 1. The magnetic induction in the specimen's plane causes a tilt of the focused electron beam, which can be detected as a shift of the beam disk by a position sensitive detector.

 0031-9007/04/93(4)/047203(4)$22.50

rings have been patterned onto a self-supporting, amorphous Si_3N_4 membrane with a thickness of approximately 30 nm and an area of $100 \times 100\ \mu m^2$. The 20 nm thick magnetic Permalloy film was deposited by thermal evaporation, the ring pattern was transferred to the Permalloy film using a Ti etch mask prepared by a combination of electron beam lithography and lift-off process and subsequent ion etching.

Two different magnetic states can be distinguished during remagnetization [11]. Minimizing the stray field energy leads to a flux closure state, where the magnetization simply follows the circumference of the ring. If an increasing external magnetic field is applied to the sample, the effect of the Zeeman energy term grows, until it is more favorable for the magnetization to adopt the direction of the external field in large areas of the specimen. This magnetic configuration was termed "onion state" [11]. Figure 2 shows a typical hysteresis loop for a single Permalloy ring with outer/inner diameters of 1.5 and 0.75 μm, respectively, and a thickness of 20 nm. The loop was recorded with a special electron microscopic image based technique [12], the magnetic configuration of certain measured points is also depicted. The fact that the loop is not closed is due to an electron gun brightness drift and specimen contamination during the long duration measurement.

In the hysteresis loop the switching between the two different states is clearly visible. The variations in the switching field values are due to the fact that this method does not measure an averaged particle behavior, which is usually gained from measurements over a large ensemble of nonidentical specimens. Instead, the hysteretic behavior of one individual particle is accessible. Coming from a saturated state, at -15.9 kA/m (-200 Oe) the particle is in the onion state. Inset (a) shows the ring uniformly bright except the domain wall regions. According to the mapping direction shown in inset (b), this corresponds to an upward pointing onion state. At 6.1 kA/m (77 Oe) the jump in the loop indicates the transformation into the flux closure state, characterized by a dark and a bright semicircle in inset (b). The reversed onion state is reached at 11.6 kA/m (146 Oe), the image (c) shows the ring in dark shades, corresponding to a downward pointing onion state. Decreasing the field again leads to a flux closure configuration at -2.3 kA/m (-29 Oe) and finally to the initial onion state at -12.6 kA/m (-158 Oe).

Micromagnetic simulations [11] show that the flux closure state is achieved only in the presence of pinning sites. Without pinning both "poles" of the onion state start to rotate simultaneously and the reversed onion state is reached without the intermediate flux closure state. Only the introduction of artificial pinning sites or symmetry breaking causes a hysteresis loop in the simulations similar to the one shown in Fig. 2. In reality, symmetry breaking is almost always present. Therefore, to accomplish switching without the intermediate flux closure state, an experimental trick has been applied: We have observed flux closure free switching experimentally in the presence of a bias field applied in plane and perpendicular to the switching field. In Fig. 3, a 3 μm/2.5 μm Permalloy ring was saturated in the positive y direction; then the external field H_y was decreased to zero and reversed, while a bias field H_x of 3.2 kA/m (40 Oe) was maintained. Although the dimensions are different from the ring in Fig. 2, without bias field a similar behavior is expected [4]. However, if the external field is lowered from the state of saturation, the "poles" start to rotate without annihilating themselves, and, if H_y is set to zero, the onion state is oriented with respect to H_x. By increasing the reversed field, the domain walls continue to rotate, until the reversed onion state is achieved without an intermediate flux closure state.

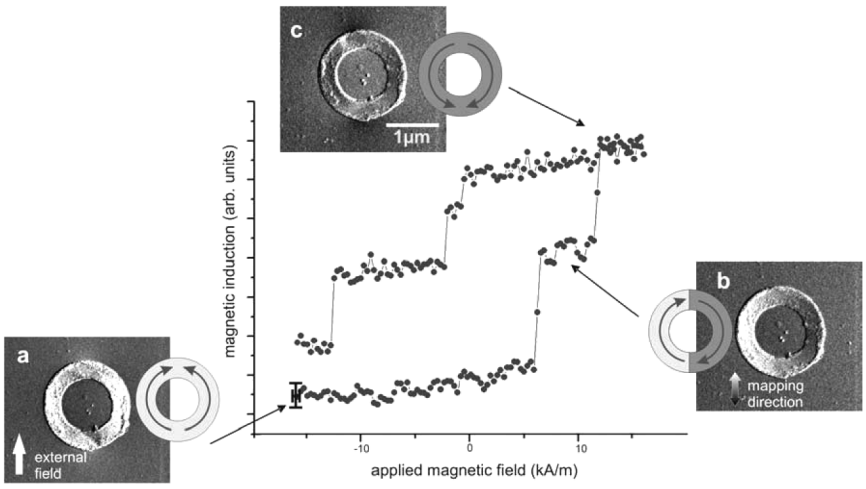

FIG. 2. A hysteresis loop of a 20 nm thick and 1.5 μm/0.75 μm diameter Permalloy ring recorded by fully automated DPC. Every measured point is calculated from an image acquired with the corresponding external magnetic field applied as described in [12]. The mapping direction is shown in inset (b).

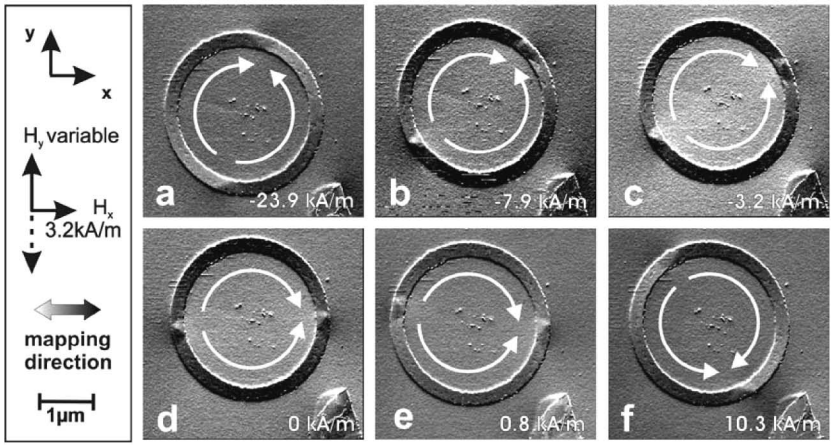

FIG. 3. A sequence of a remagnetization process without the intermediate flux closure state for a 3 μm/2.5 μm Permalloy ring with 20 nm thickness, recorded with DPC. The mapping direction is along the x axis, as indicated on the left side. The external field H_y was applied along the positive y direction, then subsequently reduced to zero and increased in the reversed direction, while a bias field H_x of 3.2 kA/m (40 Oe) was held constant. The magnetic configuration is shown by the curved arrows inside the rings. The "poles" of the onion state rotate simultaneously to form a reversed onion state in the end.

Our high resolution technique allows even more detailed insight into micromagnetism. In thin magnetic stripes "head-to-head" domain walls may exist [13], where two different types are distinguished, as sketched in the insets of Fig. 4. The first type [Fig. 4(a)] was termed a transverse wall; here the two domains are separated by an area where the magnetization is rotated by 90°. As this direction is perpendicular to the stripes's long edge, the stray field energy is enlarged. The second possibility is the introduction of a vortex core [Fig. 4(b)]. This flux closure state allows the adjacent inductions pointing "head-to head" to merge with the induction pattern of the vortex, which decreases the energy within the domain wall. However, the generation of a vortex increases the exchange energy density of the wall area.

The type of domain wall that appears thus depends on energy minimization considerations: The generation of a transverse wall is favored if the increased stray field energy is overcompensated by an energy gain in the exchange energy term, which is the main energy contribution in the vortex wall case. It was assumed that the onion state configuration in Permalloy rings leads to both domain wall types. For the first time, high resolution DPC microscopy allows the investigation of the walls, and both types of head-to-head walls are present in a ring exposed to an external field of 7.9 kA/m (−100 Oe) (see Fig. 4).

Figure 4(a) shows a transverse wall. The magnetization of the two adjacent domains points to the right and to the left side, respectively, while in the wall region the

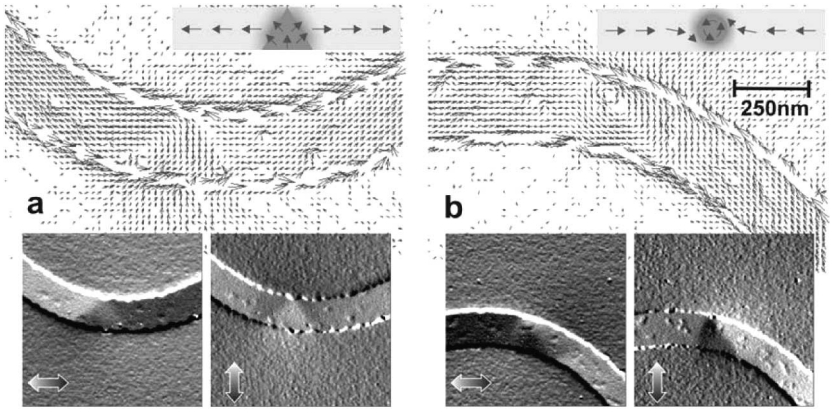

FIG. 4. High resolution images of head-to-head domain walls in a 20 nm thick ring structure in the onion state configuration at −7.9 kA/m (−100 Oe). In (a) a transverse domain wall occurs, whereas in (b) a vortex domain wall is observed. Here the two perpendicular components of the magnetic induction are displayed with the mapping direction indicated by the double-headed arrow, and a reconstructed induction vector field is shown. In the latter plot, vectors with lengths under a certain threshold have been omitted. The variations in thickness at the ring edges also cause deflection effects, which are detected as well.

magnetization is rotated and is directed radially, causing a visible stray field. The "V"-like configuration is typical for this kind of domain wall. In our case, the transverse domain wall occurs only if it is additionally assisted by an external field. If this field is lowered, also the transverse wall is transformed in a vortex wall, which seems to be the energetic lower state for the investigated 3 μm/2.5 μm Permalloy ring with 20 nm thickness. The presence of both wall types in this ring is due to the fact that the external field is within the critical field range, where the transition occurs. The vortex wall type is depicted in Fig. 4(b). A vortex separates the two adjacent domains with the magnetization pointing into the wall's direction. We have used differential phase contrast to investigate remagnetization processes in Permalloy rings. DPC allows high resolution images under applied field conditions, which makes this approach very suitable for a vast field of investigations. Thus the two expected types of domain walls could be resolved in detail. Furthermore, we were able to switch the rings from one onion state to the reversed one without the intermediate flux closure field by applying an in-plane bias field perpendicular to the switching field.

The authors would like to thank Dr. M. Schneider and M. Rahm for the instruction in the fabrication of the specimen, and Professor D. Weiss for making possible the use of his clean room facilities. This work has been supported by the German Research Society (DFG) (Forschergruppe 370 Ferromagnet-Halbleiter-Nanostrukturen).

*Email address: thomas.uhlig@physik.uni-regensburg.de

[1] J. G. Zhu, Y. Zheng, and G. A. Prinz, J. Appl. Phys. **87**, 6668 (2000).
[2] S. P. Li *et al.*, Phys. Rev. Lett. **86**, 1102 (2001).
[3] M. Kläui *et al.*, Appl. Phys. Lett. **78**, 3268 (2001).
[4] M. Kläui *et al.*, J. Phys. Condens. Matter **15**, 985(R) (2003).
[5] M. Kläui *et al.*, Phys. Rev. B **68**, 134426 (2003).
[6] J. N. Chapman, J. Phys. D **17**, 623 (1984).
[7] J. N. Chapman and M. R. Scheinfein, J. Magn. Magn. Mater. **200**, 729 (1999).
[8] M. Schneider, H. Hoffmann, and J. Zweck, Appl. Phys. Lett. **77**, 2909 (2000).
[9] J. N. Chapman, I. R. McFadyen, and S. McVitie, IEEE Trans. Magn. **26**, 1506 (1990).
[10] J. Zweck, J. N. Chapman, S. McVitie, and H. Hoffmann, J. Magn. Magn. Mater. **104–107**, 315 (1992).
[11] J. Rothman *et al.*, Phys. Rev. Lett. **86**, 1098 (2001).
[12] T. Uhlig, and J. Zweck, Ultramicroscopy **99**, 137 (2004).
[13] R. D. McMichael and M. J. Donahue, IEEE Trans. Magn. **33**, 4167 (1997).